Mark S. Ghiorso · Richard O. Sack

Chemical mass transfer in magmatic processes IV. A revised and internally consistent thermodynamic model for the interpolation and extrapolation of liquid-solid equilibria in magmatic systems at elevated temperatures and pressures

Abstract A revised regular solution-type thermodynamic model for twelve-component silicate liquids in the system SiO_2–TiO_2–Al_2O_3–Fe_2O_3–Cr_2O_3–FeO–MgO–CaO–Na_2O–K_2O–P_2O_5–H_2O is calibrated. The model is referenced to previously published standard state thermodynamic properties and is derived from a set of internally consistent thermodynamic models for solid solutions of the igneous rock forming minerals, including: (Mg, Fe^{2+}, Ca)-olivines, $(Na, Mg, Fe^{2+}, Ca)^{M2}$ $(Mg, Fe^{2+}, Ti, Fe^{3+}, Al)^{M1}$ $(Fe^{3+}, Al, Si)_2^{TET}O_6$-pyroxenes, (Na,Ca,K)-feldspars, (Mg, Fe^{2+}) $(Fe^{3+}, Al, Cr)_2O_4$-$(Mg, Fe^{2+})_2$ TiO_4 spinels and $(Fe^{2+}, Mg, Mn^{2+})TiO_3$-$Fe_2O_3$ rhombohedral oxides. The calibration utilizes over 2,500 experimentally determined compositions of silicate liquids coexisting at known temperatures, pressures and oxygen fugacities with apatite ± feldspar ± leucite ± olivine ± pyroxene ± quartz ± rhombohedral oxides ± spinel ± whitlockite ± water. The model is applicable to natural magmatic compositions (both hydrous and anhydrous), ranging from potash ankaratrites to rhyolites, over the temperature (T) range $900°$–$1700°$ C and pressures (P) up to 4 GPa. The model is implemented as a software package (MELTS) which may be used to simulate igneous processes such as (1) equilibrium or fractional crystallization, (2) isothermal, isenthalpic or isochoric assimilation, and (3) degassing of volatiles. Phase equilibria are predicted using the MELTS package by specifying bulk composition of the system and either (1) T and P, (2) enthalpy (H) and P, (3) entropy (S) and P, or (4) T and volume (V). Phase relations in systems open to oxygen are determined by directly specifying the f_{O_2} or the T-P-f_{O_2} (or equivalently H-P-f_{O_2}, S-P-f_{O_2}, T-V-f_{O_2}) evolution path. Calculations are performed by constrained minimization of the appropriate thermodynamic potential. Compositions and proportions of solids and liquids in the equilibrium assemblage are computed.

M. S. Ghiorso (✉)
Department of Geological Sciences, AJ-20,
University of Washington, Seattle, WA 98195, USA

R. O. Sack
Department of Earth and Atmospheric Sciences,
Purdue University, West Lafayette, IN 47907, USA

Editorial responsibility: T. L. Grove

Introduction and motivation

In this paper, we present a substantial revision of the thermodynamic model of Ghiorso et al. (1983) and announce new computer software for the calculation of chemical mass transfer in magmatic systems (e.g. Ghiorso 1985; Ghiorso and Carmichael 1985; Ghiorso and Kelemen 1987). Impetus to revise our earlier work began with a realization that the shortcomings of the model of Ghiorso et al. (1983) stem from a lack of internally consistent end member thermodynamic data and from inadequate models of activity-composition relations of the igneous rock-forming minerals. In preparing the revision, we have addressed these difficulties by adopting the thermodynamic database of Berman (1988), extending it to include internally consistent thermodynamic models for the relevant igneous solid solutions (Ghiorso 1990a; Ghiorso and Sack 1991; Sack and Ghiorso 1989, 1991a, b, 1994a, b, c). In addition to these improvements, the database of liquid-solid experiments upon which the liquid mixing properties are estimated has been greatly expanded in coverage of temperature, pressure and liquid composition, and new algorithms (Ghiorso and Carmichael 1987) implementing "phase-absent" constraints have been utilized in calibration. The resulting model is a robust description of the Gibbs free energy of mixing of natural silicate liquids, applicable to magmatic compositions (both hydrous and anhydrous), ranging from potash ankaratrites to rhyolites, over the temperature range $900°$–$1700°$ C and pressures up to 4 GPa.

Before discussing specific data sources and algorithms utilized in the construction of our model, it is appropriate to motivate these issues with a summary of the thermodynamic basis for calibration. We are ultimately interested in generating models which quantify the relative stability of solid and liquid phases in igneous systems. The intent is to construct multicomponent phase diagrams which account for all the major elements in the system and which are rooted in a thermodynamic formulation. The latter is essential, as our knowledge of solid-liquid equilibria in igneous systems requires both extrapolation and interpolation to encompass the full range of compositions, temperatures and pressures relevant to igneous petrogenesis. Although the Gibbs free energy of the system is the critical descriptor of phase stability, its direct calibration is unfeasible. However, experimental determination of phase compositions, equilibrated at known temperatures and pressures, serve to identify "points" in composition space of mutual tangency to the Gibbs surfaces of coexisting solid and liquid. This condition arises as a manifestation of the equality of chemical potentials in a system of heterogeneous phases which coexist in a state of equilibrium. *If* thermodynamic properties of the coexisting solids are taken as known, then in principle, an internally consistent description of the Gibbs free energy of the liquid may be derived from the experimental liquid-solid database. In practice, three sorts of complications arise: (1) solution models for solid phases may not account for all the components present in the liquid (e.g. Na or K in olivine) and consequently, will leave undefined certain critical slopes of the tangent surface of the Gibbs energy of the liquid in just those directions of composition space, (2) the experimental database may be so narrowly focused as to span a relatively small range of liquid compositions, thereby providing insufficient constraints to extrapolate the liquid Gibbs surface to other compositions of petrologic interest, and (3) the adopted solution models for the solid phases may be based upon mutually inconsistent thermodynamic properties, which introduces conflicting constraints on the derived properties of the liquid.

Ghiorso et al. (1983) encountered all three of these complications in calibrating their model for the Gibbs free energy of solution of natural silicate liquids. They addressed the first two problems by utilizing numerical techniques for extraction of model parameters which have their basis in generalized inverse theory (Lawson and Hanson 1974; Ghiorso 1983). These techniques provide numerically stable values of model parameters, but they do not resolve the issue of the limited scope of the solid-solution models employed. Consequently, chemical potentials of certain liquid components such as TiO_2, Fe_2O_3, MnO and P_2O_5 are very poorly defined by their calibration. Perhaps more importantly, Ghiorso et al. (1983) did not address the issue of internal inconsistency of end member thermodynamic prop-

erties. This led to a systematic discrepancy in modeled $Fe^{2+}(Mg)_{-1}$ exchange potentials between liquid and coexisting ferromagnesian silicates. Another symptom of the lack of an internally consistent database is poor extrapolation of certain mineral-liquid stability relations at very high or very low temperatures and at elevated pressures.

In this paper the deficiencies of the model of Ghiorso et al. (1983) are systematically addressed. We summarize first the basic thermodynamic relations and the revised and enlarged liquid-solid experimental database, describe the selection of standard state end member thermodynamic properties and solid solution models, and then develop a revised and internally consistent calibration for the liquid.

Basic thermodynamic relations and calibration method

We seek a calibration of the molar Gibbs free energy (G) of natural silicate liquids, as defined by the expression (Ghiorso et al. 1983):

$$G = \sum_{i=1}^{n} X_i \mu_i^0 + RT \sum_{i=1}^{n} X_i \ln X_i + \frac{1}{2} \sum_{i=1}^{n} \sum_{j=1}^{n} W_{i,j} X_i X_j$$
$$+ RT[X_w \ln X_w + (1 - X_w)\ln(1 - X_w)], \qquad (1)$$

where R is the gas constant, T is the temperature in absolute, X_i is the mole fraction of the ith thermodynamic component in the liquid (n is the total number of these components), X_w is the mole fraction of water, μ_i^0 is the standard state[1] chemical potential of the ith component and $W_{i,j}$ are temperature, pressure-independent "regular-solution" type interaction parameters. The last describe non-ideal solution behavior in the liquid. We assume $W_{i,j} = W_{j,i}$ and that the $W_{i,i}$ are zero. The validity of Eq. (1) in accounting for volumes and heat capacities of mixing for magmatic composition melts as well as solid-liquid phase relations and experiments on water saturation in multicomponent silicate liquids has been argued thoroughly in the literature (e.g. Ghiorso and Carmichael 1980; Nicholls 1980; Ghiorso et al. 1983; Ghiorso 1987; Kress and Carmichael 1988, 1989, 1991; Lange and Carmichael 1987, 1989, 1990; Lange and Navrotsky 1992). These arguments will not be repeated here. Our objective in calibrating Eq (1) is to find optimal values of the $W_{i,j}$. We achieve this objective by constraining compositional derivatives of $\bar{G}$ with experimental data on the compositions of silicate liquids that are saturated or under saturated with one or more solid phases ± water. The derivative of $\bar{G}$ with respect to X_k (composition) is related via Darken's equation[2] to the chemical potential, μ_k. From Eq. 1, the chemical potential of the kth component is given by:

$$\mu_k = \mu_k^0 + RT \ln X_k + \sum_{i-1}^{n} X_i W_{i,k}$$

$$- \frac{1}{2} \sum_{i=1}^{n} \sum_{j-1}^{n} W_{i,j} X_i X_j + RT \ln(1 - X_w) \qquad (2a)$$

---

[1] Unit activity of the pure substance at any temperature and pressure

[2] For Eq. (1), Darken's relation is given by $\mu_k = \bar{G} + \sum_{i=1}^{n} (\delta_{i,k} - X_i) \dfrac{\partial \bar{G}}{\partial X_i}\Big|_{T, P, X_{j \neq i}}$, where $\delta_{i,j}$ is the Kronecker delta (Ghiorso 1990b)

and for water by:

$$\mu_w = \mu_w^0 + 2RT \ln X_w + \sum_{i=1}^{n} X_i W_{i,w} - \frac{1}{2} \sum_{i=1}^{n} \sum_{j=1}^{n} W_{i,j} X_i X_j.$$ (2b)

Constraints on the liquid chemical potentials (and indirectly, the model parameters, $W_{i,j}$) are achieved by writing a statement of the law of mass action for each experimental datum that provides either (1) the composition of some phase that coexists with a liquid of known composition under imposed values of T and pressure (P) or (2) the knowledge that a particular phase is under saturated under these conditions. In general, the reaction of phase φ with the melt is described by the set of p-relations:

$$\varphi_p = \sum_{k=1}^{n} v_{p,k} c_k,$$ (3)

where φ_p refers to the pth end member component of the phase of interest (e.g. Mg_2SiO_4 in olivine), c_k refers to the formula for the kth component in the liquid, and $v_{p,k}$ to the stoichiometric reaction coefficient for the kth liquid component. From Eq. (3), the law of mass action yields

$$\Delta \bar{G}_{\varphi_p} = -A_{\varphi_p} = \Delta \bar{G}_{\varphi_p}^0 + \sum_{k=1}^{n} v_{p,k} \ln a_k - RT \ln a_{\varphi_p}$$ (4)

where $\Delta \bar{G}_{\varphi_p}$ is the Gibbs Free energy change of reaction 3, which is equal to the negative of the chemical affinity (A_{φ_p}) of the reaction and is zero at phase saturation. $\Delta \bar{G}_{\varphi_p}^0$ is the corresponding quantity in the standard state, a_k is the activity of the kth liquid component and a_{φ_p} is the activity of the pth end member in the phase (equal to one for a pure phase). Eq. 4 may be expanded and rearranged with the aid of Eq. (2) to yield an expression for calibration of the model parameters ($W_{i,j}$):

$$-\Delta \bar{G}_{\varphi_p}^0 - RT \sum_{k=1}^{n} v_{p,k} [\ln X_k + \ln(1 - X_w)]$$

$$= A_{\varphi_p} - RT \ln a_{0_p}$$

$$+ \sum_{k=1}^{n} v_{p,k} \sum_{i=1}^{n} W_{k,i} X_i - \frac{1}{2} \sum_{k=1}^{n} v_{p,k} \sum_{i=1}^{n} \sum_{j=1}^{n} W_{i,j} X_i X_j.$$ (5)

Eq. (5) is linear in A_{φ_p} and the $W_{i,j}$ but is nonlinear in a_{φ_p}. For calibration purposes, the most straightforward implementation of eq (5) is to consider the first case mentioned above, where the compositions of both the liquid and associated solid or vapor phase have been experimentally determined at some known T and P. Then, Eq. (5) may be rearranged, placing "known" quantities on the left-hand-side (l.h.s.) of the equation and the "unknowns" ($W_{i,j}$) on the right-hand-side, to yield:

$$-\Delta \bar{G}_{0_p}^0 - RT \sum_{k=1}^{n} v_{p,k} [\ln X_k + \ln(1 - X_w)] + RT \ln a_{\varphi_p}$$

$$= \sum_{i=1}^{n} \sum_{j=1}^{n} \left[\sum_{k=1}^{n} \left(v_{p,k} \delta_{k,i} X_i - \frac{1}{2} v_{p,k} X_i X_j \right) \right] W_{i,j}$$ (6)

where A_{φ_p} is taken to be zero as the assemblage is in equilibrium. Multiple statements of Eq. (6) represent a problem in *linear* least squares analysis for the parameters $W_{i,j}$. The l.h.s. of Eq. (6) becomes the dependent variable in this analysis. Now let us consider the second case, and suppose that an experimentally investigated liquid is known to be under saturated with a particular phase under specified T, P conditions. This information may also be used to constrain the liquid model parameters. In effect, the shape of the liquid Gibbs surface (and hence the $W_{i,j}$ must be consistent with the

condition that the tangent hyperplane which emanates from the liquid composition and extends throughout component space, may never intersect the Gibbs surfaces of phases in which the liquid is undersaturated. This is equivalent to the condition that A_{φ_p} in Eq. (5) be always positive. Rearranging Eq. (5), we obtain:

$$-\Delta \bar{G}_{\varphi_p}^0 - RT \sum_{k=1}^{n} v_{p,k} [\ln X_k + \ln(1 - X_w)]$$

$$= A_{\varphi_p} - RT \ln a_{\varphi_p}$$

$$+ \sum_{i=1}^{n} \sum_{j=1}^{n} \left[\sum_{k=1}^{n} \left(v_{p,k} \delta_{k,i} X_i - \frac{1}{2} v_{p,k} X_i X_j \right) \right] W_{i,j}$$ (7)

where the "unknowns" are again grouped on the right-hand-side of the expression, and this time include the a_{φ_p}. Note that the a_{φ_p} s proxy for the composition of the solid phase which identifies the minimal energetic separation of its Gibbs surface and the tangential hyperplane of the liquid. These a_{φ_p} s (or equivalently, the mole fractions of end member solid components) are unknowns because this composition has not been experimentally determined. The general method of calibration which utilizes phase absent constraints requires nonlinear least squares analysis subject to linear equality constraints and linear inequality bounds.

An approach to model calibration that takes advantage of information on both saturated and under saturated phases provides a way of exploiting the database of liquid-solid-vapor experiments to the fullest extent. Prior attempts at model calibration (Ghiorso et al. 1983) have not recognized the significance of the undersaturated condition. Acknowledging these constraints proves crucial to the calibration of a robust model for the liquid.

Enlarged and revised liquid-solid-vapor database

Experimental data utilized in the calibration of the liquid model parameters are summarized in Tables 1 and 2[3]. The database consists of compositions of coexisting glass (silicate liquid) and solid phases ($\pm$ water) equilibrated under known temperature, pressure and oxygen fugacity conditions. Table 1 summarizes data from the literature. T, P and log f_{O_2} ranges of the experiments are provided. For each literature source, the number (N) of experiments involving a particular solid are indicated as well as the standard deviation of the residuals (kJ) of these experiments resulting from the model calibration (see calibration section below).

In constructing the literature database we have searched for experimental data that meet the following minimal criteria: (1) experiments must be on silicate melts with compositions approximating those observed in nature, not simple system liquids, (2) complete compositions of coexisting solid and liquid phases must be determined, (3) the temperature and pressure of the experiment must be known, (4) there must be documentation that supports the assumption that coexisting

---

[3] These tables are available from the authors and may be obtained via anonymous FTP from internet node *fondue.geology.washington.edu*. A complete data file, including liquid and solid compositions, is also available from this server

solid and liquid phases are in chemical equilibrium, and (5) the oxygen fugacity of the experiment must be known.

We have not included experimental data collected on synthetic systems (systems where any one of the oxides SiO_2, Al_2O_3, Fe_2O_3, FeO, MgO, CaO, Na_2O, K_2O is absent). This exclusion pertains, for example to liquid-solid data on the Fe-absent "basalt" tetrahedron, and to data from two and three component systems. The reasons for this decision stem from the fact that we are interested in generating a *simple* thermodynamic model which works for *magmatic composition* liquids. It is not our objective to calibrate a formulation which accommodates the very interesting but otherwise petrologically irrelevant bounding compositional subsystems. The reason that this is an issue is because workers who have focused their efforts on thermodynamic modeling of simple melt systems (see Berman and Brown 1987, for a synthesis and review) have demonstrated that quite complicated models are required to achieve the same level of data reproducibility as simpler formulations (e.g. Eq. 1) provide in magmatic liquids. It appears to be unequivocal, that out of the chemical complexity of magmatic liquids arises a remarkable degree of energetic simplicity. Although skeptics might

argue that complications are simply swept away by fortuitous cancellation in magmatic composition melts, it remains unarguable that the best thermodynamic model for interpolation and extrapolation of experimental data is the simplest one that adequately reproduces the data on the system of interest. From a pragmatic perspective, there are simply not enough data available on all of the compositional subsystems of interest to igneous petrologists to justify formulation of a comprehensive model. Such a model could never be calibrated. Accordingly, we focus upon melts with magmatic compositions and warn the reader against using our model on silicate liquids not represented in nature.

In Table 2 we present previously unpublished results of one atmosphere crystallization experiments. These experiments were designed to expand the range of liquid compositions covered by the literature database. Starting materials were finely ground rock powders of olivine andesites, tholeiitic and alkalic basalts, basanites, minettes, tephrites, potash ankaratrites, melilitites and leucitites. Samples were ground to powder, pressed into pellets using polyvinyl alcohol as a binding agent, and welded to loops constructed of 0.13 mm Pt wire alloyed with quantities of Fe appropriate for minimizing Fe-loss from the charge. These

Fig. 1 Summary of experimental conditions for liquid-solid assemblages in the calibration database. 1,423 "anhydrous" experiments and 170 "hydrous" (water saturated) experiments are plotted.
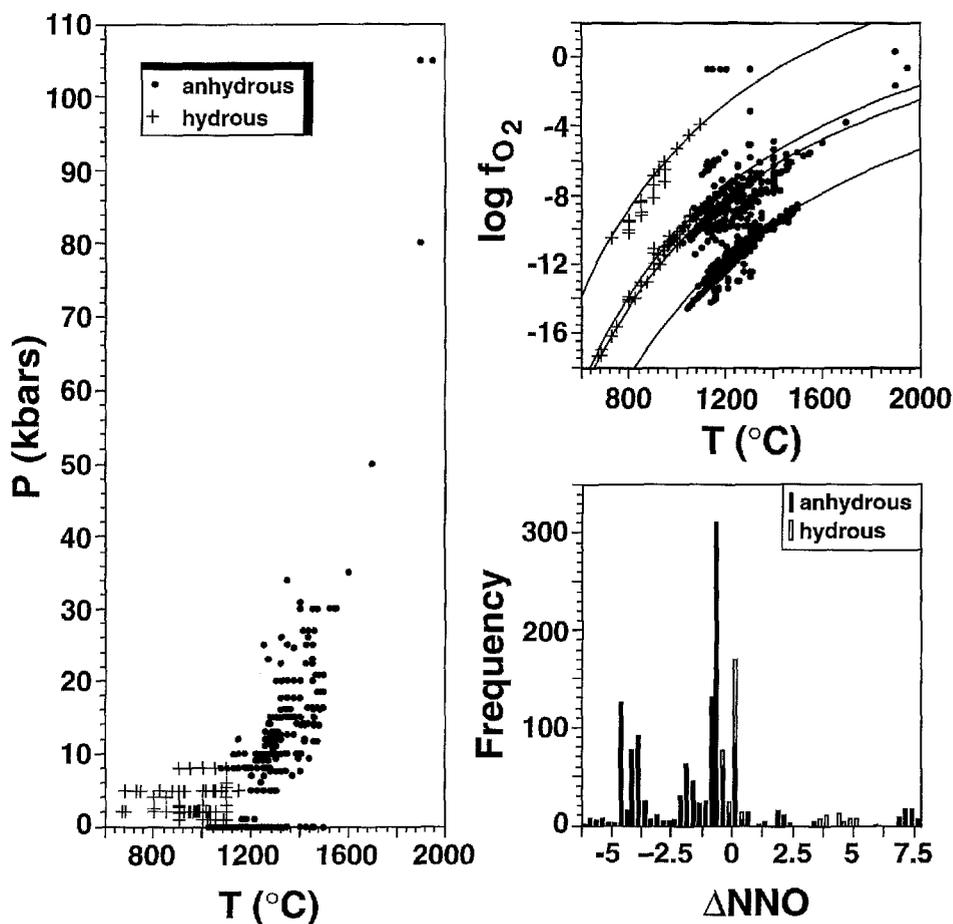
were suspended in a vertical quenching furnace, drop-quenched into water and subsequently analyzed, following the methods outlined by Sack et al. (1987) and Gee and Sack (1988). Oxygen fugacity was controlled by CO/CO_2 gas mixing or by opening the furnace to the atmosphere.

This database of liquid-solid-vapor equilibria constitutes a ten-fold increase, in turns of the number of regression equations (e.g. Eq. 6), over that used in the previous calibration (Ghiorso et al. 1983). More importantly, the current database spans the range of melt compositions represented by silicate magmatic liquids and includes T, P and $\log f_{O_2}$ conditions representative

of the crust and upper mantle. In Fig. 1 we plot intensive variables that characterize the experiments of the calibration database. Note in particular, that the range of oxygen fugacities covered by these experiments is thirteen orders of magnitude. In Fig. 2, liquid compositions from the calibration database are displayed on Le Maitre (1984) style classification diagrams.

Although greatly expanded in coverage of natural compositions, the calibration database still suffers from inadequacies. The vast majority of data have been collected upon "basalt"-like liquid compositions and have been acquired at low pressure (< 0.3 GPa). The latter is in part a consequence of the fact that

Fig. 2a, b Summary of liquid compositions for liquid-solid assemblages in the calibration database. The TAS classification scheme is after Le Maitre (1984). 1,423 "anhydrous" experiments and 170 "hydrous" (water saturated) experiments are plotted. a Anhydrous experiments. b Water-saturated experiments.
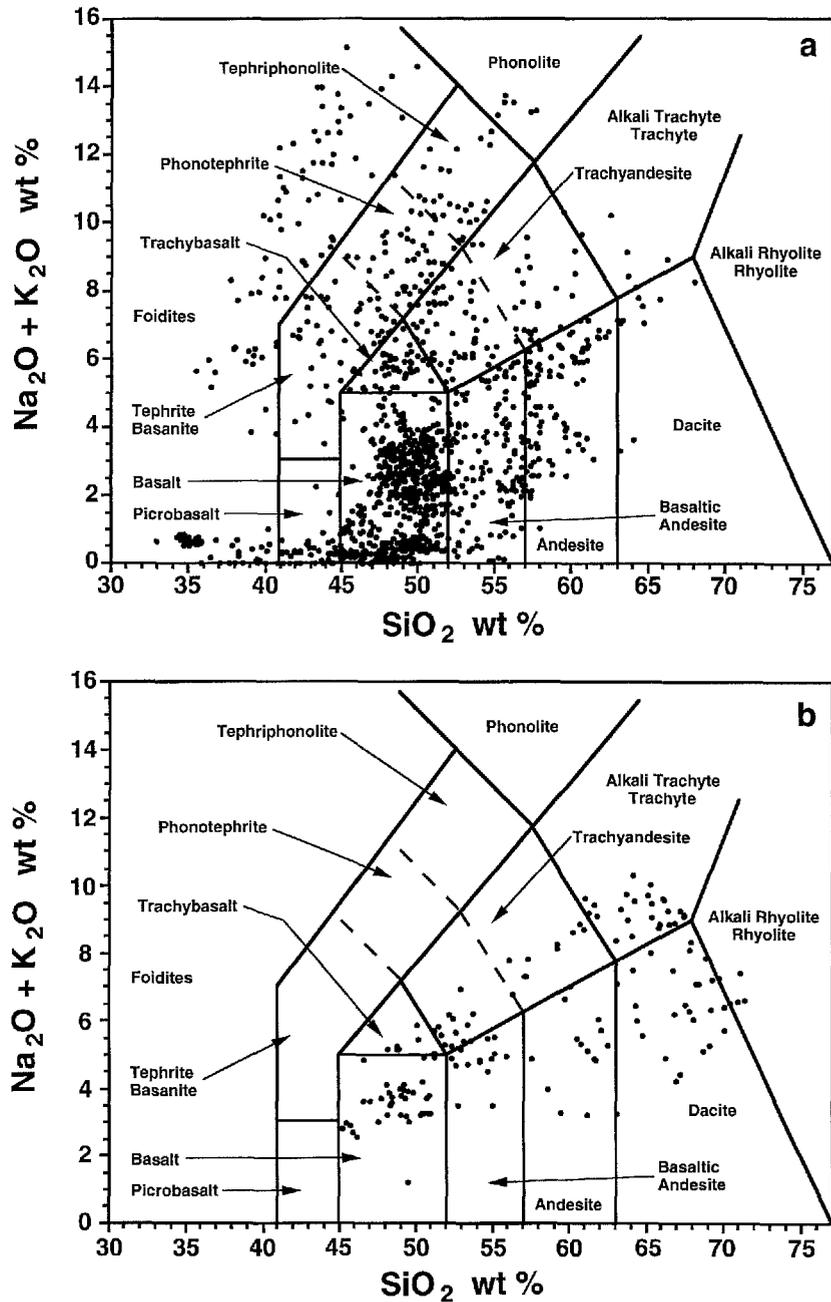
a significant fraction of published high-pressure experimental results on natural compositions are unusable for the purpose of liquid calibration. This is due either to a poorly constrained or unconstrained knowledge of oxygen fugacity (hence liquid ferric-ferrous ratio) or to an experimental geometry or duration which precluded attainment of equilibrium between liquid and solid during the run. Perhaps the greatest difficulty with the current calibration database is the absence of quantitative data (i.e. determinations of *compositions* of minerals coexisting with liquids) for water under saturated conditions and the paucity of usable data for melts containing dissolved CO_2.

End member component thermodynamic properties

Calibration of the melt interaction parameters, utilizing either Eq. (6) or (7), requires evaluation of standard state Gibbs energy changes for reactions between end member solid and liquid components. It is crucial to the success of the calibration that these end member thermodynamic properties be internally consistent, otherwise the solution interaction parameters $(W_{i,j})$ calibrated from them will be forced to accommodate relative errors in the standard state properties. We address this concern by adopting solid end member properties consistent with the database of Berman (1988). In the appendix we summarize data on the end member properties needed for calibration (Table A1), and discuss our internally consistent extensions to Berman (1988) for those end member compositions not considered in his study. In the appendix we also discuss the extension of Berman (1988) to afford calculation of Gibbs energies of end member liquid components. This extension is dictated by two criteria: (1) the liquid components *must* be chosen so as to span the composition space of natural silicate liquids with *positive* mole fractions, otherwise a more elaborate entropy of mixing model than that embodied in Eq. (1) would need to be formulated, and (2) the liquid components *should* be chosen to have stoichiometries identical to solid phases whose reference properties are tabulated by Berman (1988) and for which the enthalpy/entropy of fusion has been experimentally determined. These two criteria motivate our choice of liquid components, and these are indicated along with their thermodynamic properties in Table A1. Specific details are discussed in the Appendix.

Thermodynamic models for solid solutions

Evaluation of Eqs. (6) and (7) for the purposes of model calibration, assumes the availability of activity/composition relations for the solid phases identified in the experimental database. In order to extract self consis-

tent values of model parameters, these activity/composition relations must be internally consistent with the adopted standard state properties. For the majority of igneous solid solution series, this is not a trivial requirement, and we have expended considerable effort to achieve this goal. The problem is that the values assumed for mixing parameters in a given thermodynamic description of a mineral solution series, generally depend on the choice of thermodynamic data for the end member components of that series and often (through constraining heterogeneous phase relations) upon models for other solid solutions.

The adopted activity/composition models are internally consistent, in the sense of the previous paragraph, with the end member database of Berman (1988). They include formulations for feldspar [$CaAl_2Si_2O_8$-$(Na,K)AlSi_3O_8$; Elkins and Grove 1990], olivine [$Ca(Mg,Fe)SiO_4$-$(Mg,Fe)_2SiO_4$; Hirschmann 1991], orthopyroxene [$(Mg,Fe)_2Si_2O_6$; Sack and Ghiorso 1989], pyroxene [$(Mg,Fe^{2+})_2Si_2O_6$-$Ca(Mg,Fe^{2+})$ Si_2O_6-$CaTi_{1/2}$ $(Mg,Fe)_{1/2}(Al, Fe^{3+})SiO_6$-$Ca(Al, Fe^{3+})(Al,Fe^{3+})SiO_6$-$Na(Al,Fe^{3+})Si_2O_6$; Sack and Ghiorso 1994a,b,c), rhombohedral oxides [$(Mg,Mn, Fe^{2+})TiO_3$-$(Fe^{3+})_2O_3$; Ghiorso 1990a, Ghiorso and Sack 1991], and spinel [$(Mg,Fe^{2+})(Al,Cr,Fe^{3+})_2O_4$-$(Mg,Fe^{2+})_2TiO_4$; Sack and Ghiorso 1991a, b].

Calibration procedure and results

Model parameters are obtained by least squares analysis of a set of equations of the form of Eqs. (6) and (7) constructed from the experimental database (Tables 1 and 2), the adopted end member thermodynamic properties (Table A1) and the assumed activity-composition relations for mineral solid solutions. The chemical reactions relevant to this analysis are provided in Table 3. The indicated stoichiometric coefficients give the appropriate values of $v_{p,k}$ necessary for the evaluation of Eqs. (6) and (7). In constructing these equations, we have calculated the ferric-ferrous ratio of the liquid according to the algorithm of Kress and Carmichael (1991).

Regression equations generated from phase present or equilibrium coexistence data (e.g. Eq. 6) are linear in the model parameters, $W_{i,j}$. Equations constructed from phase absent constraints (e.g. Eq (7)) are linear in A_φ and $W_{i,j}$ but non-linear in the X_{φ_p}. Each of the imposed phase absent constraints generates an unknown reaction affinity, and a set of unknown mole fractions of end member solid components. In addition, each imposed phase absent constraint generates a bound condition that its affinity be positive and that the sum of the component mole fractions be unity. For a calibration database of respectable size, the imposition of phase absent constraints can rapidly produce a regression problem with enormous numbers

Table 3 Reactions used in calibrating the model

Phase/Component		Reaction: **solid** = liquid
Olivine	Fayalite	$Fe_2SiO_4 = Fe_2SiO_4$
	Forsterite	$Mg_2SiO_4 = Mg_2SiO_4$
Pyroxene	Diopside	$CaMgSi_2O_6 = \frac{1}{2}SiO_2 + \frac{1}{2}Mg_2SiO_4 + CaSiO_3$
	Enstatite	$Mg_2Si_2O_6 = Mg_2SiO_4 + SiO_2$
	Hedenbergite	$CaFeSi_2O_6 = \frac{1}{2}SiO_2 + \frac{1}{2}Fe_2SiO_4 + CaSiO_3$
Feldspar	Albite	$NaAlSi_3O_8 = \frac{5}{2}SiO_2 + \frac{1}{2}Al_2O_3 + \frac{1}{2}Na_2SiO_3$
	Anorthite	$CaAl_2Si_2O_8 = SiO_2 + Al_2O_3 + CaSiO_3$
	Sanidine	$KAlSi_3O_8 = 2SiO_2 + KAlSiO_4$
Quartz		$SiO_2 = SiO_2$
Tridymite		
Leucite		$KAlSi_2O_6 = SiO_2 + KAlSiO_4$
Corundum		$Al_2O_3 = Al_2O_3$
Spinel	Chromite	$FeCr_2O_4 + \frac{1}{2}Mg_2SiO_4 = MgCr_2O_4 + \frac{1}{2}Fe_2SiO_4$
	Hercynite	$FeAl_2O_4 + \frac{1}{2}SiO_2 = Al_2O_3 + \frac{1}{2}Fe_2SiO_4$
	Magnetite	$Fe_3O_4 + \frac{1}{2}SiO_2 = Fe_2O_3 + \frac{1}{2}Fe_2SiO_4$
	Spinel	$MgAl_2O_4 + \frac{1}{2}SiO_2 = Al_2O_3 + \frac{1}{2}Mg_2SiO_4$
	Ulvöspinel	$Fe_2TiO_4 + SiO_2 = TiO_2 + Fe_2SiO_4$
Rhombohedral Oxide	Geikielite	$MgTiO_3 + \frac{1}{2}SiO_2 = TiO_2 + \frac{1}{2}Mg_2SiO_4$
	Hematite	$Fe_2O_3 = Fe_2O_3$
	Ilmenite	$FeTiO_3 + \frac{1}{2}SiO_2 = TiO_2 + \frac{1}{2}Fe_2SiO_4$
Whitlockite		$Ca_3(PO_4)_2 = Ca_3(PO_4)_2$
Apatite		$Ca_5(PO_4)_3(OH) + \frac{1}{2}SiO_2 = \frac{1}{2}CaSiO_3 + \frac{3}{2}Ca_3(PO_4)_2 + \frac{1}{2}H_2O$
Water		H_2O **(liquid or gas)** = H_2O (dissolved in melt)

of equations and unknowns. For example, if 1,000 liquids in the calibration database were known to be under saturated with feldspar ($NaAlSi_3O_8$–$KAlSi_3O_8$ $CaAl_2Si_2O_8$), this would generate 3,000 statements of Eq. (7). There would be 4,066 parameters in the regression problem: 66 $W_{i,j}$, 3000 feldspar mole fractions, and 1,000 reaction affinities. The least-squares solution would be subject to 1,000 equality constraints specifying that the mole fraction sum for each "absent" feldspar be unity, and 1,000 inequality bounds imposing positivity on each of the reaction affinities. Formidable non-linear regression problems of this scale may be solved using the software package of Murtagh and Saunders (1987). Their algorithm takes advantage of the fact that most of the regression parameters (4,000 of the 4,066 in our example of feldspar) only appear in a very small number of regression equations and are coupled only through the derived values of the $W_{i,j}$. Such methods are known as techniques in sparse non-linear optimization.

We have extended the algorithm of Murtagh and Saunders (1987) to account for the high degree of correlation between the $W_{i,j}$ model parameters. Recognition of this correlation is essential if values of extracted interaction parameters are expected to be stable to extrapolation and interpolation of the calibration database. The method of extension involves first identifying the level of correlation between the "independent" variables, second constructing uncorrelated linear combinations of the $W_{i,j}$ which become the new "indepen-

dent" variables of the regression problem, and third choosing the minimal subset of these new variables that predict the dependent variable at an acceptable level of precision. This is the method of singular value analysis (SVA) which we have used previously (Ghiorso et al. 1983; Ghiorso 1983) on linear regression problems. Here, we apply the singular value method to the non-linear algorithm by solving a series of related singular value decompositions (SVD) on the subset of linear regression parameters during each step of the non-linear minimization. The algorithm is numerically stable, requires a minimal amount of computer time and storage and can accommodate a regression problem like the one described here with greater than 50,000 equations and 40,000 parameters.

In analyzing the calibration database we adopt the following procedure. An initial solution to the $W_{i,j}$ is obtained by evaluating only the phase-present (Eq. 6) constraints. This generates a linear sub problem in only 66 parameters and approximately 4,600 regression equations. The number of phase-present regression equations is restricted by including only solid-solution end members whose mole fraction exceeds 0.05 in the reported phase. Thus, an experimental determination of coexisting olivine and liquid will result in a regression equation for the Mg_2SiO_4 (forsterite) component if the mole fraction of Mg in the olivine exceeds 0.05, Fe_2SiO_4 (fayalite) if $X_{Fe} > 0.05$, and $CaMgSiO_4$ if $X_{Mg}^{M1} > 0.05$ and $X_{Ca}^{M2} > 0.05$. This restriction assures that compositional uncertainties at low concentrations

do not overwhelm the model calibration. We solve the linear regression sub problem using SVA. This procedure identifies and resolves correlations between the independent variables. The solution to this linear problem is used as an initial guess to the larger non-linear regression problem which incorporates the phase-absent constraints. We analyze the larger problem using the modified algorithm of Murtagh and Saunders (1987). The solution of the non-linear problem serves to identify *active* phase absent-constraints, i.e. a constraint whose derived affinity is zero, indicating apparent saturation. The active phase-absent constraints are then individually examined and relaxed within an "uncertainty window" estimated from residuals on phase-present equations involving the same phase. For example, if the standard deviation of residuals associated with fitting leucite-present data is 1 kJ, then an uncertainty window of $\pm$ 2 kJ ($\pm$ 2 σ) is applied to the leucite absent equations. The logic here is that at the 2σ level, the leucite saturation surface cannot be determined to better than 2 kJ by the model and consequently, enforcement of phase absent criteria must recognize this statistical uncertainty. The calibration procedure is deemed to converge when there are fewer than 2.2% (one-tailed 2σ probability) active phase absent constraints outside of the uncertainty window. The entire calibration procedure is software driven and is available as part of the MELTS package, described below.

Optimal values of the model parameters are provided in Table 4. Residuals on the phase-present equations are categorized by phase and data source in Fig. 3 and are enumerated in Table 1. For simplicity, we have grouped residuals for solid solution end members by averaging each experiment and computing a standard deviation of the averages. This representation is adequate in that individual end member residuals show no systematic bias with respect to the mean, i.e. the average residual on each end member in a solid solution is approximately that of the solid solution as a whole. Average residuals for individual experiments are *not* correlated, but end member residuals within a given phase/experiment are highly correlated. This is

to be expected, and removal of this correlation motivates our choice for reporting residuals in Fig. 3 and Table 1. The number of regression equations of each type of phase-present constraint is also indicated in the Table. Note that in Fig. 3, the brackets are four standard deviations wide and are centered about the average error for that phase/data source. The overall standard deviation of residuals is 2.72 kJ in the dependent variable (l.h.s. of Eq. 6) on 4,666 statements of phase-present constraints. If we remove the within experiment correlation (as above), this value drops to 1.3 kJ on 2,540 experiments. This translates roughly to an ability to back-predict the liquidus temperature of a given experiment to within 10° or equivalently, to calculate the composition of the liquidus phase to within 3 mol%.

The important generalizations to be reached from the analysis of residuals of the model calibration are that (1) the average residual and standard deviation of residuals for each phase are on the whole comparable to that of the overall regression, and that (2) the within-in-phase variation of residuals shows no obvious correlation to experimental study. The first generalization demonstrates the absence of inter-phase systematic bias and is violated only for the silica minerals (Fig. 3). We suspect that there may be equilibration problems in the high-pressure experiments involving quartz and that the offset in tridymite residuals may be mostly attributed to a systematic bias in modeling the activity of SiO_2 in the extremely iron rich liquids from which this phase precipitated. The latter would point to a deficiency in model formulation. Alternatively, these systematic offsets may offer evidence that the adopted
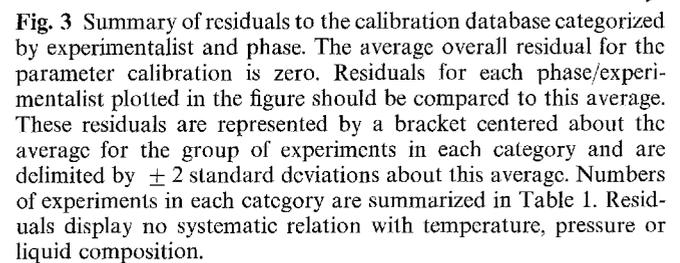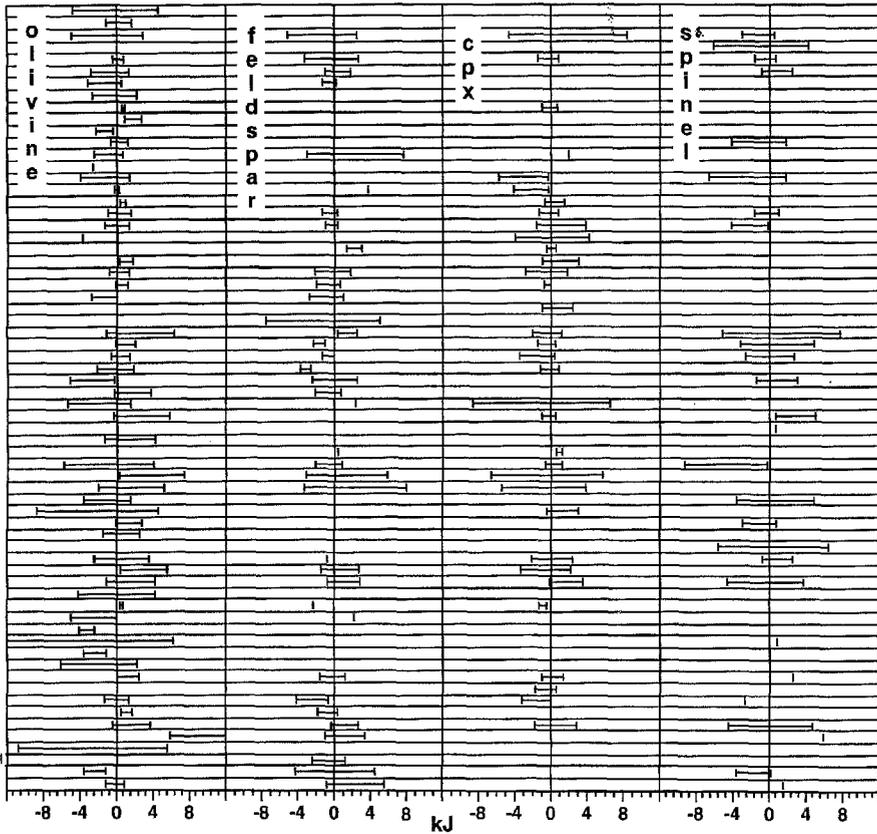
Fig. 3 Summary of residuals to the calibration database categorized by experimentalist and phase. The average overall residual for the parameter calibration is zero. Residuals for each phase/experimentalist plotted in the figure should be compared to this average. These residuals are represented by a bracket centered about the average for the group of experiments in each category and are delimited by $\pm$ 2 standard deviations about this average. Numbers of experiments in each category are summarized in Table 1. Residuals display no systematic relation with temperature, pressure or liquid composition.
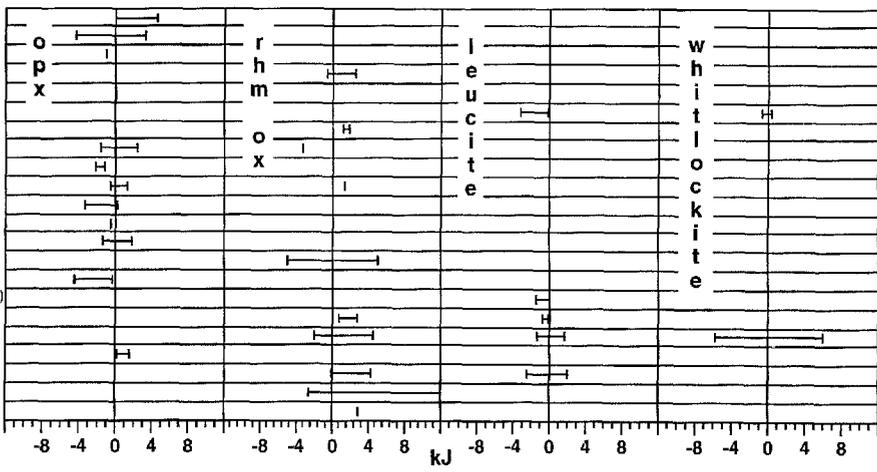
Table 4 Regular solution interaction parameters for the liquid phase (values in kJ)

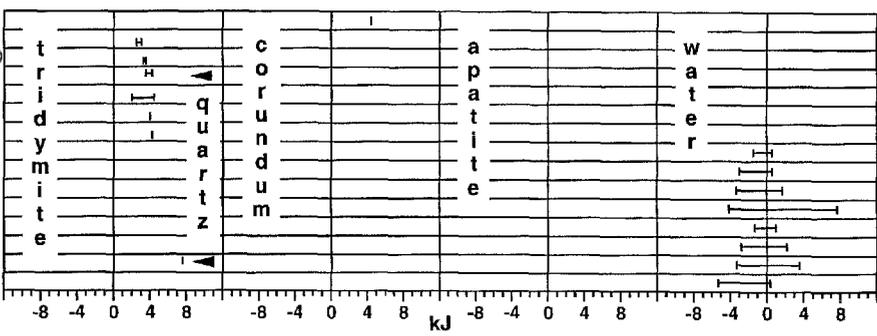|	SiO$_2$	TiO$_2$	Al$_2$O$_3$	Fe$_2$O$_3$	MgCr$_2$O$_4$	Fe$_2$SiO$_4$	Mg$_2$SiO$_4$	CaSiO$_3$	Na$_2$SiO$_3$	KAlSiO$_4$	Ca$_3$(PO$_4$)$_2$	H$_2$O
SiO$_2$												
TiO$_2$	26267											
Al$_2$O$_3$	− 39120	− 29450										
Fe$_2$O$_3$	8110	− 84757	− 17089									
MgCr$_2$O$_4$	27886	− 72303	− 31770	21606								
Fe$_2$SiO$_4$	23661	5209	− 30509	− 179065	− 82972							
Mg$_2$SiO$_4$	3421	− 4178	− 32880	− 71519	46049	− 37257						
CaSiO$_3$	− 864	− 35373	− 57918	12077	30705	− 12971	− 31732					
Na$_2$SiO$_3$	− 99039	− 15416	− 130785	− 149662	113646	− 90534	− 41877	− 13247				
KAlSiO$_4$	− 33922	− 48095	− 25859	57556	75709	23649	22323	17111	6523			
Ca$_3$(PO$_4$)$_2$	61892	25939	52221	− 4214	5342	87410	− 23209	37070	15572	17101		
H$_2$O	30967	81879	− 16098	31406		28874	35634	20375	− 96938	10374	43451	

Top panel — author list (left axis):

Agee & Walker (1990)
Arndt (1977)
Baker & Eggler (1987)
Barnes (1986)
Bartels & Grove (1991)
Bartels et al. (1991)
Bender et al. (1978)
Bickle (1978)
Biggar et al. (1971)
Chen et al. (1982)
Delano (1977)
Delano (1980)
Fram & Longhi (1992)
Fujii & Bougalt (1983)
Gee & Sack (1988)
Grove & Beaty (1980)
Grove & Bence (1977)
Grove & Bryan (1983)
Grove & Juster (1989)
Grove & Lindsley (1979)
Grove & Raudsepp (1978)
Grove & Vaniman (1978)
Grove et al. (1982)
Grove et al. (1990)
Grove et al. (1993)
Hess et al. (1978)
Johnson (1986)
Jurewicz et al. (1993)
Juster et al. (1989)
Kennedy et al. (1990)
Kinzler & Grove (1985)
Kinzler & Grove (1992)
Leeman (1974)
Longhi & Pan (1988)
Longhi & Pan (1989)
Longhi et al. (1974)
Longhi et al. (1978)
Longhi et al. (1983)
Mahood & Baker (1986)
Meen (1987)
Meen (1990)
Murck & Campbell (1986)
Nielsen et al. (1988)
Rhodes et al. (1979)
Roeder (1974)
Roeder & Reynolds (1991)
Sack & Carmichael (1984)
Sack & Ghiorso (1994c)
Sack et al. (1987)
Seifert et al. (1988)
Stolper (1977)
Stolper (1980)
Takahashi (1980)
Takahashi (1986)
Takahashi & Kushiro (1983)
Thompson (1974, 1975)
Tormey et al. (1987)
Treiman (1989)
Ussler & Glazner (1989)
Walker et al. (1973)
This Paper
Helz (1976)
Kelemen et al. (1990)
Luhr (1990); Housh & Luhr (1991)
Sisson & Grove (1992a)
Sisson & Grove (1992b)

Panel labels: olivine | feldspar | cpx | sp & spinel

Axis: -8 -4 0 4 8 | -8 -4 0 4 8 kJ | -8 -4 0 4 8 | -8 -4 0 4 8

Middle panel — author list:

Baker & Eggler (1987)
Barnes (1986)
Biggar et al. (1971)
Delano (1980)
Fram & Longhi (1992)
Gee & Sack (1988)
Grove & Beaty (1980)
Grove & Juster (1989)
Grove et al. (1982)
Juster et al. (1989)
Longhi & Pan (1988)
Longhi & Pan (1989)
Longhi et al. (1983)
Mahood & Baker (1986)
Meen (1987)
Sack & Carmichael (1984)
Sack & Ghiorso (1994c)
Sack et al. (1987)
Ussler & Glazner (1989)
This Paper
Helz (1976)
Kelemen et al. (1990)

Panel labels: opx | rhm ox | leucite | whitlockite

Axis: -8 -4 0 4 8 | -8 -4 0 4 8 kJ | -8 -4 0 4 8 | -8 -4 0 4 8

Bottom panel — author list:

Fram & Longhi (1992)
Grove & Lindsley (1979)
Grove & Raudsepp (1978)
Johnson (1986)
Longhi & Pan (1988)
Stolper (1977)
Walker et al. (1973)
Burnham & Jahns (1962)
Hamilton et al. (1964)
Helz (1976)
Khitarov et al. (1959)
Luhr (1990)
Naney (1983)
Sisson & Grove (1992a)
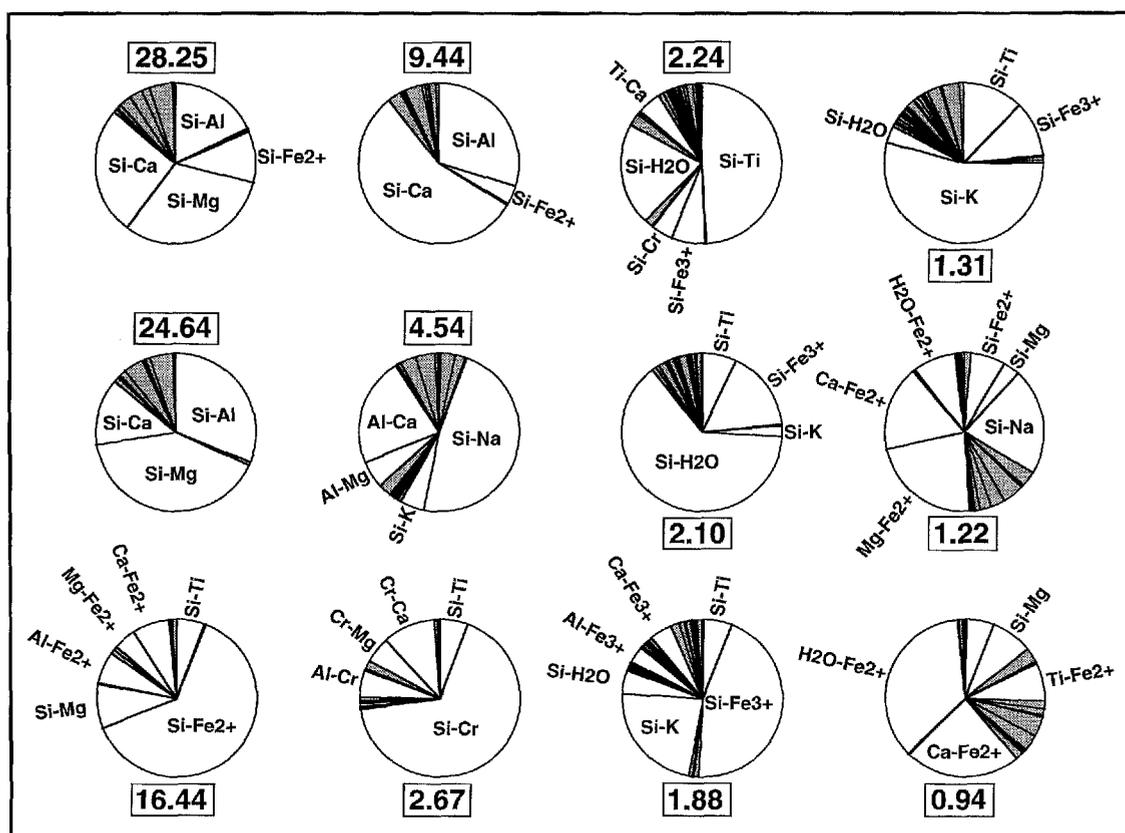Sisson & Grove (1992b)

Panel labels: tridymite | corundum quartz | apatite | water

Axis: -8 -4 0 4 8 | -8 -4 0 4 8 kJ | -8 -4 0 4 8 | -8 -4 0 4 8

temperature dependence to the heat capacity of the SiO_2 liquid component (see appendix) may be inappropriate for natural composition melts; the temperature spread of the tridymite saturation experiments is very small and averages about $1000°$ C below the fusion temperature of cristobalite. It is even possible that the appreciable alkali contents of natural tridymites may be the origin of this energetic offset. There are too few data on silica mineral-melt saturation to pursue a solution to this puzzle. From the second generalization we conclude that residuals for a given phase are not particularly sensitive to variations in experimental

conditions. These include temperature, pressure, bulk composition and methods or standards used for microprobe analysis. In this regard it is worth emphasizing, that unlike our previous model calibrations (Ghiorso et al. 1983), no experimental data were arbitrarily excluded from the fitting procedure on the basis of poor quality of fit.

From a statistical perspective, not all 66 model parameters reported in Table 4 are of equal importance to a solution of the regression problem. A quantitative understanding of the significance of the various parameters may be gleaned by examining a singular value decomposition (SVD) produced during the final stage of calibration. As described above, SVD reassembles the model parameters into an equal number of linear combinations or eigenvectors. These eigenvectors are constructed so that each represents a truly independent or uncorrelated fraction of the variance of the independent variables. Moreover, the fraction of variance accounted by each of the eigenvectors is provided in the analysis. In Fig. 4 we display a representation of the first twelve eigenvectors of the model calibration presented here. Each eigenvector is represented by a pie-diagram. The numeric label attached to each pie corresponds to the percentage of the *total* variance accounted for by that eigenvalue. The first twelve eigenvectors displayed in Fig. 4 account for 95% of the total variance of the independent variables. The pie wedges indicate the proportion of variance attributable to each

Fig. 4 Visual representation of the Singular Value Decomposition (SVD) of the parameter calibration matrix constructed from the calibration database. Each pie diagram denotes an independent variable of the parameter calibration problem with the significance (% variance) of that variable indicated as a numeric value displayed above or below each pie. The wedges of each pie indicate the relative contribution of each liquid regular solution interaction parameter ($W_{i,j}$ in the text). All 66 $W_{i,j}$s contribute to each pie diagram, with only the dominant contributions labeled. Minor contributions are *shaded*. Mutually dominant $W_{i,j}$s *within* a given pie diagram indicate a high degree of statistical correlation. The wedges are labeled using the following scheme: (1) Si, Ti, Al, Fe3$^+$, Cr, Fe2$^+$, Mg, Ca, Na, K, H2O refer to the liquid components SiO_2, TiO_2, Al_2O_3, Fe_2O_3, $FeCr_2O_4$, Fe_2SiO_4, Mg_2SiO_4, $CaSiO_3$, Na_2SiO_3, $KAlSiO_4$ and H_2O respectively, and (2) a $W_{i,j}$ is indicated by the symbol i-j, i.e. W_{SiO_2,Al_2O_3} is denoted Si-Al. There are a total of 66 independent linear combinations of the $W_{i,j}$, but only the first 12 are shown. These constitute over 95% of the total variance in the calibration database.

of the model parameters. Thus, the principal eigenvector accounts for 28.25% of the total variance and is mainly composed of contributions from W_{SiO_2, Al_2O_3}, W_{SiO_2, Mg_2SiO_4}, W_{SiO_2, Fe_2SiO_4}, and $W_{SiO_2, CaSiO_3}$. Fig. 4 reveals that the most dominant and consequently most statistically secure of the calibrated interaction parameters are the ones which constitute the eigenvectors of highest variance. These involve mainly interactions with the SiO_2 component, which is not surprising, as SiO_2 has more variability than any other compositional variable. Additionally, Fig. 4 demonstrates the extent of parameter correlation; parameters corresponding to dominant pie wedges in a given pie diagram are highly correlated. These correlations are not always immediately intuitive in that they cannot be easily interpreted in terms of simple solid-liquid reaction stoichiometry. Our final model calibration is constructed from 56 eigenvectors of the possible 66 $W_{i,j}$ combinations. This cutoff accounts for 99% of the allowable variance. The $W_{i,j}$ parameters are reconstructed from these 56 eigenvectors following standard SVA methods (Lawson and Hanson 1974).

The MELTS software package

The best way to demonstrate the consequences of the parameter calibration discussed above is to utilize the derived coefficients to forward model crystal-liquid equilibria of well known bulk compositions. This has the advantage of displaying the consequences of the calibration in terms of calculated liquidi, phase compositions and proportions — much more familiar concepts than uncertainties in end member chemical potentials. To facilitate calculations of this sort we have developed MELTS, a new software package for modeling chemical mass transfer in magmatic systems. MELTS is based upon algorithms for energy minimization described by Ghiorso et al. (1983), Ghiorso (1985), and Ghiorso and Kelemen (1987) and incorporates new procedures for determination of the saturation state and stability of strongly nonideal solid solutions with respect to silicate melt (Ghiorso 1994). It supersedes and expands the capabilities of the previously released modeling software, SILMIN. Capabilities of the MELTS package include (1) revising and/or updating the parameter calibration for the liquid (using the methods outlined above) on the basis of new or revised calibration datasets, (2) modeling equilibrium or fractional crystallization of specified bulk compositions, (3) modeling crystallization paths under constrained T-f_{O_2}, total enthalpy, total entropy, total volume or any combination of these constraints, and (4) modeling assimilation or magma mixing in evolving magmatic systems. The MELTS software package may be obtained via anonymous FTP from internet node *fondue.geology.washington.edu*. MELTS is intended to be run interactively on a "UNIX"-level workstation. It utilizes an X11/Motif menu-driven graphical user interface and is written in ANSI C.

Future directions

The MELTS software package has been designed with the aim of automating the process of model recalibration and facilitating the incorporation or revision of new thermodynamic models for solid phases. Conse-

quently, revision of the model calibration presented in this paper is inevitable as new experimental data become available and as new internally consistent thermodynamic formulations for solid phases are built upon the adopted standard state database (Table A1). Furthermore, such revisions may be accomplished by users of the MELTS package. Significant improvements in the present calibration await high-quality experimental data on compositions of liquid and solid phases equilibrated at elevated pressure under conditions of known oxygen fugacity. The calibration database is still too highly skewed toward anhydrous low-pressure experiments and there is a real need for experiments in water-bearing systems, particularly involving water undersaturated melts. Improvements in the crystallization simulations await construction of a thermodynamic model for high-Ca igneous amphiboles, the formulation of a model for ternary feldspars that incorporates temperature and compositionally induced symmetry transformations, and the development of internally consistent solution theory for the feldspathoid minerals. These extensions are under development. One extremely productive future direction of MELTS involves incorporation of trace element partitioning between liquid and solid. Hirschmann and Ghiorso (1994) have begun to pursue this avenue of research by extending the calibration proposed here to model Ni, Co and Mn partitioning between liquid and olivine. Their approach is very successful in systematizing and extrapolating trace element distribution coefficients over a wide-range of temperatures and compositions. The key to the incorporation of trace elements into MELTS is the description of trace element energetics in the solid solution. Coupled substitutions and cation ordering in the solid lead to highly complex liquid/solid partitioning behavior. High quality experimental data on liquid-solid distribution coefficients, collected over a broad range of compositions and temperatures (e.g. Nielsen et al. 1994), are required but are not sufficient to achieve a generic model. Equal attention must be directed at understanding the crystal chemical constraints of trace element substitution in the solid itself. Future research on the energetics of trace element substitution in pyroxenes and spinels is prerequisite to extending MELTS to include a generic trace element partitioning model for igneous systems.

Appendix

Summary of adopted thermodynamic data

Thermodynamic data for end member solid components are taken for the most part from Berman (1988). Internally consistent extensions to this database are summarized in Table A1. Apparent molar Gibbs free energies of formation of solid end members are calculated from the tabulated quantities according Eqs 6, 13 and 20 of Berman (1988). The reference temperature (T_r) is taken to be 298 K and the reference pressure (P_r) 1 bar (0.0001 GPa).

The adopted thermodynamic properties of perovskite have not been evaluated for internal consistency with Berman (1988). The reference enthalpy and entropy of Berman's (1988) anorthite $(CaAl_2Si_2O_8)$ have been adjusted, using the calorimetric data of Carpenter (1988), in order to evaluate the properties of *metastable* $C\bar{1}$ anorthite. This is necessary, as the compositional dependence of the $I\bar{1} - > C\bar{1}$ phase transition in plagioclase is not accounted for in solution theory for the feldspars modeled by Elkins and Grove (1990) and adopted in this paper. Accepting Berman's (1988) anorthite in conjunction with Elkins and Grove's (1990) model without making this correction, has the effect of destabilizing the calcium component of the feldspar, particularly when X_{An} is greater than 0.8. The thermodynamic properties of water are calculated according to an algorithm devised by Berman (1988, personal communication.). This algorithm is based upon the Haar equation of state.

Apparent molar Gibbs energies of formation of liquid components are calculated according to

$$\Delta \bar{G}^0_{app,T,P} = \Delta \bar{H}^0_{f,T_r,P_r} + \int_{T_r}^{T_{fusion}} \bar{C}^{0,sol}_{P_r} dT + T_{fusion} \Delta \bar{S}^0_{fusion}$$

$$+ \int_{T_{fusion}}^{T} \bar{C}^{0,liq}_{P_r} dT - T \left(\bar{S}^0_{T_r,P_r} + \int_{T_r}^{T_{fusion}} \frac{\bar{C}^{0,sol}_{P_r}}{T} dT \right)$$

$$+ \Delta \bar{S}^0_{fusion} + \int_{T_{fusion}}^{T} \frac{\bar{C}^{0,liq}_{P_r}}{T} dT \right) + \Delta \bar{G}^0_{t,T,P}$$

$$+ \left[\bar{V}^0 + \left(\frac{\partial \bar{V}^0}{\partial T}\right)_P (T - 1673) \right](P - P_r) + \left[\left(\frac{\partial \bar{V}^0}{\partial P}\right)_T \right.$$

$$+ \left(\frac{\partial^2 \bar{V}^0}{\partial T \partial P}\right)(T - 1673) \right]\left(\frac{P^2}{2} - P_r P + \frac{P_r^2}{2}\right)$$

$$+ \left(\frac{\partial^2 \bar{V}^0}{\partial P^2}\right)\left(\frac{P^3}{6} - \frac{P_r P^2}{2} + \frac{P_r^2 P}{2} - \frac{P_r^3}{6}\right)$$

where the properties of the solid are determined as above. By this method, thermodynamic properties of the liquid components are anchored to those of the indicated solid phases (Table A1). With the exception of the unadjusted calorimetrically determined values for Na_2SiO_3 (sodium metasilicate), the latter are internally consistent with Berman (1988). We have adopted entropies of fusion from a number of sources and in some cases have estimated values from correlation algorithms (see Stebbins et al. 1984 and footnotes to Table A1). Note in particular, our adopted value for the entropy of fusion of forsterite, 57.2 J/K. This value is based upon an *estimate* of the enthalpy of fusion of forsterite published by Navrotsky et al. (1989), which is in turn derived from data on the enthalpy of solution of molten $CaAl_2Si_2O_8–Mg_2SiO_4$ liquids at 1500° C. Our value differs from that reported by Navrotsky et al. (1989; 53 ± 9 J/K) in that we have adjusted their calculations to reflect our adopted values of the heat capacities of both forsterite and Mg_2SiO_4 liquids. Within the expected uncertainty of ± 9 J/K, our adopted value is consistent with the lower bound (65.3 ± 6 J/K) of the recently published measurement of Richet et al. (1993).

The paucity of data on entropies of fusion of geologically relevant materials forces us to adopt a number of values which are little more than educated guesses and could have attached uncertainties on the order of 20% of the indicated value. In the context of the model proposed in this paper however, we think these estimates are adequate for two reasons: (1) estimates of $\Delta \bar{S}^0_{fusion}$ in conjunction with our adopted model for the entropy of mixing in the liquid, allow us to reproduce many of the measured entropies of fusion of more complex compounds, and (2) these estimates are highly correlated to the derived values of the excess enthalpy of mixing of the liquid and are therefore, rendered internally consistent by model calibration to the adopted reference set of solid properties. Another way of expressing this consistency is to note that we see no temperature dependence to the residuals of any solid-liquid equilibrium relations over a range of temperatures that span 800° C. However, it is important to realize that the estimated values of $\Delta \bar{S}^0_{fusion}$ tabulated in A1, and in fact many of the calorimetrically determined values reported in this table, may only be internally consistent with Berman (1988) when used in conjunction with our proposed model. *Caveat emptor.*

Liquid heat capacities tabulated in Table A1 are obtained largely from the algorithms of Lange and coworkers (Lange and Carmichael 1990; Lange and Navrotsky 1992) and are to be understood as partial molar heat capacities of the end member component in "magmatic" composition liquids. Note that the adopted heat capacity of molten SiO_2 is modeled as temperature dependent below 1480 K (the glass transition temperature) following Richet et al. (1982). We have incorporated this temperature dependence into our model in order to avoid a logical inconsistency that is inherent to our earlier calibration (Ghiorso et al. 1983). Simple extrapolation of the liquid properties of molten silica down from the fusion point using a constant C_P results in the liquid being more stable than the solid (quartz, tridymite or cristobalite) at temperatures below about 1200° C. One might argue from this observation that temperature dependent heat capacities should be adopted for all the "liquid" components below their respective glass transition temperatures. However, the glass transition temperature is unknown for most of the adopted components and in practice the correction between the C_P for the metastable "super cooled liquid" (the constant C_P) and that of the glass is inconsequential with respect to the total energy difference between solid and metastable "liquid". In the case of SiO_2, the illogical result manifests from the fact that the temperature integral of the heat capacity difference between glass and super-cooled liquid is of the same order as the enthalpy of fusion.

Volumetric properties of the liquid are from Lange and Carmichael (1990) and Kress and Carmichael (1991), except for values of $(\partial^2 \bar{V}^0/\partial P^2)$. These have been estimated (V. C. Kress, personal communication) by visually comparing volumetric properties calculated from

$$\bar{V}^0_{T_r,P} = \bar{V}^0_{T_r,P_r} + \left(\frac{\partial \bar{V}^0}{\partial P}\right)_T (P - P_r) + \left(\frac{\partial \bar{V}^0}{\partial P}\right)_T \left(\frac{P^2}{2} - P_r P + \frac{P_r^2}{2}\right)$$

to those calculated from the Birch–Murnaghan equation

$$\bar{V}^0_{T_r,P} = \frac{3K}{2}\left[\left(\frac{\bar{V}^0_{T_r,P_r}}{\bar{V}^0_{T_r,P}}\right)^{\frac{7}{3}} - \left(\frac{\bar{V}^0_{T_r,P_r}}{\bar{V}^0_{T_r,P}}\right)^{\frac{5}{3}}\right]$$

$$\times \left\{1 - \frac{3(4 - K')}{4}\left[\left(\frac{\bar{V}^0_{T_r,P_r}}{\bar{V}^0_{T_r,P}}\right)^{\frac{2}{3}} - 1\right]\right\}$$

Here K is defined for each liquid component as

$$K = \frac{\bar{V}^0_{T_r,P_r}}{\left(\frac{\partial \bar{V}^0}{\partial P}\right)_T}$$

Table A1 Additional thermodynamic properties of endmember solids and liquids. Volumetric properties of the liquid are from Lange and Carmichael (1990) and data for the solids are from Berman (1988) unless footnoted

Solid Phase	Formula	ΔH^0_f[h]	S^0(J/K)	V^0(J/bar)	k_0	$k_1 \times 10^{-2}$	$k_2 \times 10^{-5}$	$k_3 \times 10^{-7}$	$v_1 \times 10^6$	$v_2 \times 10^{12}$	$v_3 \times 10^6$	$v_4 \times 10^{10}$	T_t(K)	ΔH_t[h]	$l_1 \times 10^2$	$l_2 \times 10^5$
Clinoenstatite	$Mg_2Si_2O_6$	-3081636[a]	137.570[a]	6.330[a]	333.16	-24.012	-45.412	55.830	-0.749	0.447	24.656	74.670				
Hedenbergite[a]	$CaFeSi_2O_6$	-2845389	171.431	6.789	307.89	-15.973	-69.925	93.522	-0.993	1.4835	31.371	83.672				
Alumino-Buffonite[b]	$CaTi_{1/2}Mg_{1/2}AlSiO_6$	-3275265	143.745	6.356	297.50	-13.5596	-67.022	75.908	-0.870	2.171	22.250	52.863				
Buffonite[b]	$CaTi_{1/2}Mg_{1/2}FeSiO_6$	-2836709	176.557	6.722	303.91	-14.1767	-43.565	35.252	-0.870	2.171	22.250	52.863				
Essenite[b]	$CaFeAlSiO_6$	-2860211	158.991	6.722	317.11	-17.333	-51.097	54.222	-0.870	2.171	22.250	52.863				
Anorthite	$CaAl_2Si_2O_8$	-4213249[c]	207.223[c]	10.075	439.37	-37.341	-31.702		-1.272	3.176	10.918	41.985				
Sodium-metasilicate	Na_2SiO_3	-1561427[d]	113.847[d]		234.77[e]	-22.189[e]		13.530[e]								
Nepheline[f]	$NaAlSiO_4$	-2087976	124.200	5.422	205.24	-7.599	-108.383	208.182	-2.221	600.0	31.552	0.2	467.15	241.835	-102.784	339.448
Kalsilite[f]	$KAlSiO_4$	-2111814	133.965	5.989	186.00		-131.067	213.893	-1.567	0.0	23.487	140.257	800.15	1154	-7.0965	21.682
Leucite[f]	$KAlSi_2O_6$	-3012026	210.704	9.263	271.14	-9.441	-78.572	95.920	-1.557	1.274	12.517					
Perovskite[r]	$CaTiO_3$	-1660630[g]	93.640[g]	3.363[g]	150.49[e]	-6.213[c]	-43.010[e]						1530[b]	2301.2[h]		
Chromite[f]	$FeCr_2O_4$	-1445490	142.676	4.401[g]	236.874	-16.796	-16.765									
Hercynite[i]	$FeAl_2O_4$	-1947681	115.362	4.075	235.190	-14.370	-46.913	64.564								
Ulvospinel[t]	Fe_2TiO_4	-1488500	185.447	4.682[g]	249.63	-18.174	-5.453									
Geikielite[j]	$MgTiO_3$	-1572560	74.560	3.086[g]	146.20	-4.160	-39.998	40.233	-0.584	1.230	27.248	29.968				
Hematite	Fe_2O_3	-822000[j]	87.400[j]	3.027	146.86		-55.768	52.563	-0.479	0.304	38.310	1.650	955	1287	-7.403	27.921
Pyrophanite[k]	$MnTiO_3$	-1350707[l]	104.935[m]	3.170	150.00	-4.416	-33.237	34.815	-0.584	1.230	27.248	29.968				
Whitlockite[n]	$Ca_3(PO_4)_2$	-4097169[n]	235.978[n]	9.762[b]	402.997[n]	-28.084[p]	-32.623[p]	44.794					1373[p]	14059[p]	2.5427[p]	19.255[p]
Apatite[n]	$Ca_5(PO_4)_3OH$	-6694689	398.740	16.403	758.81	-64.806										

Liquid Component	Reference Solid Phase	T_{fusion}[i]	ΔS^0_{fusion}(J/K)	C^0_p(J/K)	V^0(J/bar) at 1673 K	$\left(\dfrac{\partial V^0}{\partial T}\right)_P \times 10^4$	$\left(\dfrac{\partial V^0}{\partial P}\right)_T \times 10^5$	$\left(\dfrac{\partial^2 V^0}{\partial P \partial T}\right)_T \times 10^8$	$\left(\dfrac{\partial^2 V^0}{\partial P^2}\right)_T \times 10^{10}$
SiO_2	(amorphous)	1999[q]	4.46[q]	81.373[q]	2.690	0.0	-1.89	1.3	3.6[r]
TiO_2	rutile	1870[s]	35.824[s]	109.2[t]	2.316	7.246	-2.310	2.7	5.0[r]
Al_2O_3	corundum	2320[s]	48.61[s]	170.3[t]	3.711	2.62	-2.26	3.1	4.0[r]
Fe_2O_3	hematite	1895[s]	60.41[u]	240.9[g]	4.213	9.09	-2.53	1.8[x]	4.4[r]
$MgCr_2O_4$	picrochromite	2673[v]	73.22[v]	335.1[x]	5.358[x]	1.171[x]	-2.26[x]		4.7[r]
Fe_2SiO_4	fayalite	1490[y]	59.9[y]	240.2	5.420	5.84	-2.79	-2.3	14.6[r]
Mg_2SiO_4	forsterite	2163[z]	57.2[aa]	271.0	4.980	5.24	-1.35	-1.3	4.1[r]
$CaSiO_3$	pseudowollastonite	1817[bb]	31.5[bb]	172.4	4.347	2.92	-1.55	-1.6	3.9[r]
Na_2SiO_3	sodium metasilicate	1361[y]	38.34[y]	180.2	5.568	7.41	-4.29	-5.3	8.4[r]
$KAlSiO_4$	kalsilite	2023[cc]	24.5[dd]	217.0	6.838	7.27	-6.40	-4.6	12.1[z]
$Ca_3(PO_4)_2$	whitlockite	1943[cc]	35.690[gg]	574.7[ff]					
H_2O[hh]	(liquid)								

[a]Sack and Ghiorso (1994b); [b]Sack and Ghiorso (1994c); [c]Berman (personal communiation), additional first order phase transition in nepheline: T_t = 1180.15 K, ΔH_t = 2393 J; [d]Stull and Prophet (1971); [e]Berman and Brown (1985); [f]Berman (1988); [g]Robie et al. (1978); [h]H ref [h] from Berman (1988) adjusted to reflect I1 → C1 transition (Carpenter, 1988); T_t = 1180.15 K, ΔH_t = 1480 K, ΔH_f = 2393 J; [i]Ghiorso (1990a); [j]Naylor and Cook (1946); [k]Berman (1988), analogy with $FeTiO_3$; [l]Estimated in conjunction with Ghiorso and Sack (1991); [m]Stephenson and Smith (1968); [n]Zhu and Sverjensky (1991); [o]Southard and Milner (1935); [p]Fitted to data tabulated by Kelley (1960); [q]Richet et al. (1982); ΔH^0_f = -901554, S^0 = 48.475, below 1480 K, $\bar{C}^0_p = 127.3 - 10.777 \times 10^{-3} T + 4.3127 \times 10^5/T^2 - 463.8/\sqrt{T}$; [r]Estimated, see text; [s]Samsonov (1982); [t]Lange and Navrotsky (1992); [u]estimated from Robie et al.'s (1978) data on ΔS_{fusion} of Fe_3O_4 and FeO; [v]Levin et al. (1964); [w]estimated a posteriori by examination of temperature dependent calibration residuals on $FeCr_2O_4$-rich spinels; [x]properties taken as identical to those of $MgFe_2O_4$; [y]Stebbins et al. (1984); [z]Bowen and Anderson (1914); [aa]corrected value, based upon data in Navrotsky et al. (1989); [bb]estimated by Stebbins et al. (1984); [cc]Morse (1980, p. 257); [dd]estimated by Stebbins et al. (1984); [ee]Weast (1972); [ff]estimated from data on liquid CpS of $Ca_2P_2O_7$ and CaP_2O_6 (Weast, 1972); [gg]estimated as the average ΔS^0_{fusion} of $Mg_3(PO_4)_2$ (Weast, 1972) and $Ba_3(PO_4)_2$ (Weast, 1972); [hh]see text

and K' is taken to be 5 (Kress and Carmichael 1991). The Birch-Murnaghan equation provides an excellent means of extrapolating the volumetric properties of liquids to quite elevated pressures. However, it is non-linear in volume, which makes its use in thermodynamic formulations cumbersome. The optimal values of $(\partial^2 \bar{V}^0/\partial P^2)$ reported in Table A1 allow our simplified polynomial representation of liquid volumes to reproduce results calculated from the Birch-Murnaghan equation to pressures in excess of 4 GPa. Extension of the higher order pressure derivative of volume to the model of Lange and Carmichael (1990) was necessitated in order to maintain modeled liquid densities to be less than those of associated solid phases at pressures up to 4 GPa.

Thermodynamic properties of the H_2O component in molten silicate liquids are modeled following the method of Nicholls (1980; Ghiorso et al. 1983). We adopt his value for the reference state entropy (152.63 J/mol-K) and optimize a value of the reference enthalpy (−279.992 kJ/mol) to satisfy best the experimental data on water solubility discussed above. We modify Nicholls' (1980) function for the volume integral contribution to the molar Gibbs energy of dissolved H_2O by subtracting the Gibbs energy of supercritical water tabulated by Robie et al. (1978) and adding the identical quantity from Berman (1988, see previous paragraphs). This insures the thermodynamic properties of the H_2O component of Table A1 are internally consistent with those of the supercritical fluid.

References

Adamkovičová K, Kosa L, Proks I (1980) The heat of fusion of calcium silicate. Silikaty 24:193–201

Agee CB, Walker D (1990) Aluminum partitioning between olivine and ultrabasic silicate liquid to 6 GPa. Contrib Mineral Petrol 105:243–254

Arndt NT (1977) Partitioning of nickel between olivine and ultrabasic and basic komatiite liquids. Carnegie Inst Washington Yearb 76:553 557

Baker DR, Eggler DH (1987) Compositions of anhydrous and hydrous melts coexisting with plagioclase, augite, and olivine or low-Ca pyroxene from 1 atm to 8 kbar: applications to the Aleutian volcanic center of Atka. Amer Mineral 72:12–28

Barnes SJ (1986) The distribution of chromium among orthopyroxene, spinel and silicate liquid at atmospheric pressure. Geochim Cosmochim Acta 50:1889–1909

Bartels KS, Grove TL (1991) High-pressure experiments on magnesian eucrite compositions: constraints on magmatic processes in the eucrite parent body. Proc Lunar Planet Sci Conf 21:351–365

Bartels KS, Kinzler RJ, Grove TL (1991) High-pressure phase relations of primitive high-aluminum basalts from Medicine Lake Volcano, Northern California. Contrib Mineral Petrol 108:253–270

Bender JF, Hodges FN, Bence AE (1978) Petrogenesis of basalts from the FAMOUS area: experimental study from 0 to 15 kbars. Earth Planet Sci Letts 41:277–302

Berman RB (1988) Internally-consistent thermodynamic data for minerals in the system Na_2O-K_2O-CaO-MgO-FeO-Fe_2O_3-Al_2O_3-SiO_2-TiO_2-H_2O-CO_2. J Petrol 29:445–522

Berman RG, Brown TH (1985) Heat capacity of minerals in the system Na_2O-K_2O-CaO-MgO-FeO-Fe_2O_3-Al_2O_3-SiO_2-TiO_2-H_2O-CO_2: representation, estimation, and high temperature extrapolation. Contrib Mineral Petrol 89:168–183

Berman RG, Brown TH (1987) Development of models for multicomponent melts: Analysis of synthetic systems, In: Carmichael ISE, Eugster HP, (eds). Thermodynamic modeling of geological materials: minerals, fluids and melts (Reviews in Mineralogy vol. 17). Mineralogical society of America, Washington DC, pp 405–442

Bickle MJ (1978) Melting experiments on peridotitic komatiites, Progress in Experimental Petrology. NERC 4th Progress Rept, (NERC Publ. Series D) 11:187–195

Biggar GM, O'Hara MJ, Peckett A, Humphries DJ (1971) Lunar lavas and the achondrites: Petrogenesis of protohypersthene basalts in the maria lava lakes. Proc Lunar Planet Sci Conf 2:617–643

Bowen NL, Andersen O (1914) The binary system MgO-SiO_2. Am J Sci 37:487–500

Burnham CW, Jahns RH (1962) A method for determining the solubility of water in silicate liquids. Am J Sci 260:721 745

Carpenter M (1988) Thermochemistry of aluminum/silicon ordering in feldspar minerals, In: Salje EKH (ed.) Physical properties and thermodynamic behavior of minerals. Reidel, Dordrecht, pp 265 323

Chen H-K, Delano JW, Lindsley DH (1982) Chemistry and phase relations of VLT volcanic glasses from Apollo 14 and Apollo 17. Proc Lunar Planet Sci Conf 13 (J Geophys Res 87 Supplement):A171–A181

Delano JW (1977) Experimental melting relations of 63545, 76015, and 76055. Proc Lunar Planet Sci Conf 8:2097–2123

Delano JW (1980) Chemistry and liquidus phase relations of Apollo 15 red glass: Implications for the deep lunar interior. Proc Lunar Planet Sci Conf 11:251–288

Elkins LT, Grove TL (1990) Ternary feldspar experiments and thermodynamic models. Am Mineral 75:544–559

Fram MS, Longhi J (1992) Phase equilibria of dikes associated with Proterozoic anorthosite complexes. Am Mineral 77:605–616

Fujii T, Bougalt H (1983) Melting relations of an abyssal tholeiite and the origin of MORBs. Earth Planet Sci Lett 62:283–295

Gee LL, Sack RO (1988) Experimental petrology of melilite nephelinites. J Petrol 29:1233–1255

Ghiorso MS (1983) LSEQIEQ: A FORTRAN IV subroutine package for the analysis of multiple linear regression problems with possibly deficient pseudorank and linear equality and inequality constraints. Computers and Geosciences 9:391–416

Ghiorso MS (1985) Chemical mass transfer in magmatic processes I. Thermodynamic relations and numerical algorithms. Contrib Mineral Petrol 90:107–120

Ghiorso MS (1987) Modeling magmatic systems: Thermodynamic relations. In: Carmichael ISE, Eugster HP (eds) Thermodynamic modeling of geological materials: minerals, fluids and melts. (Reviews in Mineralogy vol 17). Mineralogical Society of America, Washington. DC, pp 443–465

Ghiorso MS (1990a) Thermodynamic properties of hematite-ilmenite-geikielite solid solutions. Contrib Mineral Petrol 104:645–667

Ghiorso MS (1990b) The application of the Darken equation to mineral solid solutions with variable degrees of order-disorder. Amer Mineral 75:539–543

Ghiorso MS (1994) Algorithms for the estimation of phase stability in heterogeneous thermodynamic systems. Geochim Cosmochim Acta (in press)

Ghiorso MS, Carmichael ISE (1980) A regular solution model for met-aluminous silicate liquids: applications to geothermometry, immiscibility, and the source regions of basic magmas. Contrib Mineral Petrol 71:323–342

Ghiorso MS, Carmichael ISE (1985) Chemical mass transfer in magmatic processes. II. Applications in equilibrium crystallization, fractionation and assimilation. Contrib Mineral Petrol 90:121–141

Ghiorso MS, Carmichael ISE (1987) Modeling magmatic systems: petrologic applications. In: Carmichael ISE, Eugster HP (eds) Thermodynamic modeling of geological materials: minerals, fluids and melts. (Reviews in Mineralogy vol. 17) Mineralogical Soceity of America, Washington DC, pp 467–499

Ghiorso MS, Kelemen PB (1987) Evaluating reaction stoichiometry in magmatic systems evolving under generalized thermodynamic constraints: examples comparing isothermal and isenthalpic assimilation. In: Mysen BO (ed) Magmatic processes: Physicochemical principles. (Geochem Soc Sp Publ 1) Geochem Soc, Penn state university, pp 319–336

Ghiorso MS, Sack RO (1991) Fe-Ti oxide geothermometry: thermodynamic formulation and the estimation of intensive variables in silicic magmas. Contrib Mineral Petrol 108:485–510

Ghiorso MS, Carmichael ISE, Rivers ML, Sack RO (1983) The Gibbs free energy of mixing of natural silicate liquids; an expanded regular solution approximation for the calculation of magmatic intensive variables. Contrib Mineral Petrol 84:107–145

Grove TL, Beaty DW (1980) Classification, experimental petrology and possible volcanic histories of the Apollo 11 high-K basalts. Proc Lunar Planet Sci Conf 11:149 177

Grove TL, Bence AE (1977) Experimental study of pyroxene-liquid interaction in quartz normative basalt 15597. Proc Lunar Planet Sci Conf 8:1549–1579

Grove TL, Bryan WB (1983) Fractionation of pyroxene-phyric MORB at low pressure: an experimental study. Contrib Mineral Petrol 84:293–309

Grove TL, Juster TC (1989) Experimental investigations of low-Ca pyroxene stability and olivine-pyroxene-liquid equilibria at 1-atm in natural basaltic and andesitic liquids. Contrib Mineral Petrol 103:287–305

Grove TL, Lindsley DH (1979) An experimental study on the crystallization of pyroxferroite. Proc Lunarr Planet Sci Conf 10:470–472

Grove TL, Raudscpp M (1978) Effects of kinetics on the crystallization of quartz normative basalt 15597: An experimental study. Proc Lunar Planet Sci Conf 9:585–599

Grove TL, Vaniman DT (1978) Experimental petrology of very low Ti (VLT) basalts. In: Mare Crisium: The view from Luna 24. Pergamon, New York, pp 445–471

Grove TL, Gerlach DC, Sando TW (1982) Origin of calc-alkaline series lavas at Medicine Lake Volcano by fractionation, assimilation, and mixing. Contrib Mineral Petrol 84:160–182

Grove TL, Kinzler RJ, Bryan WB (1990) Natural and experimental phase relations of lavas from Serocki Volcano. Proc Ocean Drill Prog Sci Res 106/107:9–17

Grove TL, Kinzler RJ, Bryan WB (1993) Fractionation of mid-ocean ridge basalt (MORB). In: Mantle flow and melt generation at mid-ocean ridges Geophys Monogr Am Geophys Union, 71:281–310

Hamilton DL, Burnham CW, Osborn EF (1964) The solubility of water and effects of oxygen fugacity and water content on crystallization in mafic magmas. J Petrol 5:21–39

Helz RT (1976) Phase relations of basalts in their melting range at $P_{H_2O} = 5$ kb as a function of oxygen fugacity. Part II. Melt compositions. J Petrol 17:139–193

Hess PC, Rutherford MJ, Campbell HW (1978) Ilmenite crystallization in nonmare basalt: genesis of KREEP and high-Ti mare basalt. Proc Lunar Planet Sci Conf 9:705–724

Hirschmann M (1991) Thermodynamics of multicomponent olivines and the solution properties of $(Ni,Mg,Fe)_2SiO_4$ and $(Ca,Mg,Fe)_2SiO_4$ olivines. Amer Mineral 76:1232–1248

Hirschmann M, Ghiorso MS (1994) Chemical potentials of $NiSi_{0.5}O_2$, $CoSi_{0.5}O_2$, and $MnSi_{0.5}O_2$ in magmatic liquids and applications to olivine-liquid partitioning. Geochim Cosmochim Acta 58:4109–4126

Housh TB, Luhr JF (1991) Plagioclase-melt equilibria in hydrous systems. Am Mineral 76:477–492

Johnson AD (1986) Anhydrous P-T phase relations of near-primary high-alumina basalt from the South Sandwich Islands: Implications for the origin of island arcs and tonalite-trondhjemite series rocks. Contrib Mineral Petrol 92:368–382

Jurewicz AJG, Mittlefehldt DW, Jones JH (1993) Experimental partial melting of the Allende (CV) and Murchison (CM) chondrites and the origin of asteroidal basalts. Geochim Cosmochim Acta 57:2123 2139

Juster TC, Grove TL, Perfit MR (1989) Experimental constraints on the generation of FeTi basalts, andesites, and rhyodacites at the Galapagos Spreading Center, 85° W and 95° W. J Geophys Res 87:9521–9274

Kelemen PB, Joyce DB, Webster JD, Holloway JR (1990) Reaction between ultramafic rock and fractionating basaltic magma. II. Experimental investigation of reaction between olivine tholeiite and harzburgite at 1150 1050°C and 5 kb. J Petrol 31:99 134

Kelley KK (1960) Contributions to the data on theoretical metallurgy: part 13, High temperature heat content, heat capacity and entropy data for the elements and inorganic compounds. US Bur Mines Bull 584

Kennedy AK, Grove TL, Johnson RW (1990) Experimental and major element constraints on the evolution of lavas from Lihir Island, Papua New Guinea. Contrib Mineral Petrol 104:772–734

Khitarov NI, Lebedev EB, Regarten EV, Arseneva RV (1959) Solubility of water in basaltic and granitic melts. Geochemistry 5:479–492

Kinzler RJ, Grove TL (1985) Crystallization and differentiation of Archean komatiite lavas from northeast Ontario: phase equilibrium and kinetic studies. Am Mineral 70:40–51

Kinzler RJ, Grove TL (1992) Primary magmas of mid-ocean ridge basalts, 1, experiments and methods. J Geophys Res 97:6885–6906

Kress VC, Carmichael ISE (1988) Stoichiometry of the iron oxidation reaction in silicate melts. Amer Mineral 73:1267–1274

Kress VC, Carmichael ISE (1989) The lime-iron-silicate melt system: redox and volume systematics. Geochim Cosmochim Acta 53:2883–2892

Kress VC, Carmichael ISE (1991) The compressibility of silicate liquids containing Fe_2O_3 and the effect of composition, temperature, oxygen fugacity and pressure on their redox states. Contrib Mineral Petrol 108:82–92

Lange RA, Carmichael ISE (1987) Densities of $Na_2O-K_2O-CaO-MgO-FeO-Fe_2O_3-TiO_2-SiO_2$ liquids: new measurements and derived partial molar properties. Geochim Cosmochim Acta 51:2931–2946

Lange RA, Carmichael ISE (1989) Ferric-ferrous equilibria in $Na_2O-FeO-Fe_2O_3-SiO_2$ melts: effects of analytical techniques on derived partial molar volumes. Geochim Cosmochim Acta 53:2195–2204

Lange RA, Carmichael ISE (1990) Thermodynamic properties of silicate liquids with emphasis on density, thermal expansion and compressibility. In: Nicholls J, Russell JK (eds.) Modern methods of igneous petrology: understanding magmatic processes (Reviews in Mineralogy vol. 24) Minerological Society of America, Washington DC, pp 25–59

Lange RA, Navrotsky A (1992) Heat capacities of Fe_2O_3-bearing silicate liquids. Contrib Mineral Petrol 110:311–320

Lawson CL, Hanson RJ (1974) Solving least squares problems. Prentice-Hall, Englewood Cliffs, New Jersey

Le Maitre RW (1984) A proposal by the IUGS subcommission on the systematics of igneous rocks for a chemical classification of volcanic rocks based on the total alkali silica (TAS) diagram. Aust J Earth Sci 31:243–255

Leeman WP (1974) Part I. Petrology of basaltic lavas from the Snake River plain, Idaho and Part II. Experimental determination of partitioning of divalent cations between olivine and basaltic liquid. PhD dissertation, Geology, Univ Oregon

Levin EM, Robbins CR, McMurdie HF (1964) Phase diagrams for ceramists. American Ceramic Society, Colombus, Ohio

Longhi J, Pan V (1988) A reconnaisance study of phase boundaries in low-alkali basaltic liquids. J Petrol 29:115–147

Longhi J, Pan V (1989) The parent magmas of the SNC meteorites. Proc Lunar Planet Sci Conf 19:451–464

Longhi J, Walker D, Grove TL, Stolper EM, Hays JF (1974) The petrology of the Apollo 17 mare basalts. Proc Lunar Planet Sci Conf 5:447–469

Longhi J, Walker D, Hays JF (1978) The distribution of Fe and Mg between olivine and lunar basaltic liquids. Geochim Cosmochim Acta 42:1545–1558

Longhi J, Wooden JL, Pan V (1983) The petrology of high-Mg dikes from the Beartooth Mountains, Montana: a search for the parental magma of the Stillwater Complex. Proc Lunar Planet Conf, 14 Part I (J Geophys Res 88 Supplement):B53–B69

212

Luhr JF (1990) Experimental phase relations of water- and sulfur-saturated arc magmas and the 1982 eruptions of El Chichón volcano. J Petrol 31:1071–1114

Mahood GA, Baker DR (1986) Experimental constraints on depths of fractionation of midly alkalic basalts and associated felsic rocks: Pantelleria, Strait of Sicily. Contrib Mineral Petrol 93:251–264

Meen JK (1987) Formation of shoshonites from calcalkaline basalt magmas: geochemical and experimental constraints from the type locality. Contrib Mineral Petrol 97:333–351

Meen JK (1990) Elevation of potassium content of basaltic magma by fractional crystallization: the effect of pressure. Contrib Mineral Petrol 104:309–331

Morse SA (1980) Basalts and phase diagrams. Springer, Heidelberg

Murck BW, Campbell IH (1986) The effects of temperature, oxygen fugacity and melt composition on the behavior of chromium in basic and ultrabasic melts. Geochim Cosmochim Acta 50:1871–1888

Murtagh BA, Saunders MA (1987) MINOS 5.1 User's Guide. Stanford Univ, Dept Operations Research, Technical Report SOL 83 20R

Naney MT (1983) Phase equilibria of rock-forming ferromagnesian silicates in granitic systems. Am J Sci 283:993–1033

Navrotsky A, Ziegler D, Oestrike R, Maniar P (1989) Calorimetry of silicate melts at 1773 K: measurement of enthalpies of fusion and of mixing in the systems diopside-anorthite-albite and anorthite-forsterite. Contrib Mineral Petrol 101:122–130

Naylor BF, Cook OA (1946) High-temperature heat contents of metatitanates of calcium, iron, and magnesium. J Am Chem Soc 68:1003

Nicholls J (1980) A simple model for estimating the solubility of H_2O in magmas. Contrib Mineral Petrol 74:211–220

Nielsen RL, Davidson PM, Grove TL (1988) Pyroxene-melt equilibria: an updated model. Contrib Mineral Petrol 100:361–373

Nielsen RJ, Forsythe LM, Gallahan WE, Fisk MR (1994) Major and trace element magnetite-melt equilibria. Chem Geol (in press)

Rhodes JM, Lofgren GE, Smith DP (1979) One atmosphere melting experiments on ilmenite basalt 12008. Proc Lunar Planet Sci Conf 5:407–422

Richet P, Bottinga Y, Denielou L, Petitet JP, Tequi C (1982) Thermodynamic properties of quartz, cristobalite and amorphous SiO_2: drop calorimetry measurements between 1000 and 1800 K and a review from 0 to 2000 K. Geochim Cosmochim Acta 46:2639–2658

Richet P, Leclerc F, Benoist L (1993) Melting of forsterite and spinel, with implications for glass transition of Mg_2SiO_4 liquid. Geophys Res Letts 20:1675–1678

Robie RA, Hemingway BS, Fisher JR (1978) Thermodynamic properties of minerals and related substances at 298.15 K and 1 bar (10^5 Pascals) pressure and at higher temperature. US Geol Surv Bull 1452

Roeder PL (1974) Activity of iron and olivine solubility in basaltic liquids. Earth Planet Sci Lett 23:397–410

Roeder PL, Reynolds I (1991) Crystallization of chromite and chromium solubility in basaltic melts. J Petrol 32:909–934

Sack RO, Carmichael ISE (1984) $Fe^{2+} \leftrightarrow Mg^{2+}$ and $TiAl_2/MgSi_2$ exchange reactions between clinopyroxenes and silicate melts. Contrib Mineral Petrol 85:103–115

Sack RO, Ghiorso MS (1989) Importance of considerations of mixing properties in establishing an internally consistent thermodynamic database: thermochemistry of minerals in the system Mg_2SiO_4-Fe_2SiO_4-SiO_2. Contrib Mineral Petrol 102:41–68

Sack RO, Ghiorso MS (1991a) An internally consistent model for the thermodynamic properties of Fe-Mg-titanomagnetite-aluminate spinels. Contrib Mineral Petrol 106:474–505

Sack RO, Ghiorso MS (1991b) Chromian spinels as petrogenetic indicators: thermodynamics and petrological applications. Amer Mineral 76:827–847

Sack RO, Ghiorso MS (1994a) Thermodynamics of multicomponent pyroxenes: I. Formulation of a general model. Contrib Mineral Petrol 116:277–286

Sack RO, Ghiorso MS (1994b) Thermodynamics of multicomponent pyroxenes: II. Applications to phase relations in the quadrilateral. Contrib Mineral Petrol 116:287–300

Sack RO, Ghiorso MS (1994c) Thermodynamics of multicomponent pyroxenes: III. Calibration of $Fe^{2+}(Mg)_{-1}$, $TiAl(MgSi)_{-1}$, $TiFe^{3+}(MgSi)_{-1}$, $AlFe^{3+}(MgSi)_{-1}$, $NaAl(CaMg)_{-1}$, $Al_2(MgSi)_{-1}$ and $Ca(Mg)_{-1}$ exchange reactions between pyroxenes and silicate melts. Contrib Mineral Petrol (in press)

Sack RO, Walker D, Carmichael ISE (1987) Experimental petrology of alkalic lavas: constraints on cotectics of multiple saturation in natural basic liquids. Contrib Mineral Petrol 96:1–23

Samsonov GV (1982) The Oxide handbook, 2nd edn. IFI/Plenum, New York

Seifert S, O'Neill HStC, Brey G (1988) The partitioning of Fe, Ni and Co between olivine, metal, and basaltic liquid: an experimental and therrmodynamic investigation, with application to the composition of the lunar core. Geochim Cosmochim Acta 52:603–615

Sisson TW, Grove TL (1992a) Experimental investigations of the role of H_2O in calc-alkaline differentiation and subduction zone magmatism. Contrib Mineral Petrol 113:143–166

Sisson TW, Grove TL (1992b) Temperatures and H_2O contents of low-MgO high-alumina basalts. Contrib Mineral Petrol 113:143–166

Southard JC, Milner RT (1935) Low temperature specific heats. V. The heat capacity of tricalcium phosphate between 15 and 298° K. J Am Chem Soc 57:983–984

Stebbins JF, Carmichael ISE, Moret LK (1984) Heat capacities and entropies of silicate liquids and glasses. Contrib Mineral Petrol 86:131–148

Stephenson CC, Smith D (1968) Heat capacity of manganese titanate from 30° to 300° K. J Chem Phys 49:1814–1818

Stolper EM (1977) Experimental petrology of eucrite meteorites. Geochim Cosmochim Acta 41:587–611

Stolper EM (1980) A phase diagram for mid-ocean ridge basalts: preliminary results and implications for petrogenesis. Contrib Mineral Petrol 74:13–27

Stull DR, Prophet H (1971) JANAF Thermochemical tables, 2nd edn. Nat Stand Ref Data Ser Nat Bur Stand 37

Takahashi E (1980) Melting relations of an alkali-olivine basalt to 30 kbars, and their bearing on the origin of alkali basalt magmas. Carnegie Inst Washington Yearb 79:271–276

Takahashi E (1986) Melting of dry peridotite KLB-1 up to 14 GPa: implications on the origin of peridotitic upper mantle. J Geophys Res 91:9367–9382

Takahashi E, Kushiro I (1983) Melting of dry peridotite at high pressures and basalt magma genesis. Am Mineral 68:859–879

Thompson RN (1974) Primary basalts and magma genesis I. Contrib Mineral Petrol 45:317–345

Thompson RN (1975) Primary basalts and magma genesis II. Contrib Mineral Petrol 52:213–232

Tormey DR, Grove TL, Bryan WB (1987) Experimental petrology of normal MORB near the Kane Fracture Zone: 22°–25° N, mid-Atlantic ridge. Contrib Mineral Petrol 96:121–139

Treiman AH (1989) An alternate hypothesis for the origin of Angra dos Reis: porphyry, not cumulate. Proc Lunar Planet Sci Conf 9:443–450

Ussler III W, Glazner AF (1989) Phase equilibria along a basalt-rhyolite mixing line: implications for the origin of calc-alkaline intermediate magma. Contrib Mineral Petrol 101:232–244

Walker D, Grove TL, Longhi J, Stolper EM, Hays JF (1973) Origin of lunar feldspathic rocks. Earth Planet Sci Lett 20:325–336

Walker D, Shibata T, DeLong SE (1979) Abyssal tholeiites from the Oceanographer fracture zone. II. Phase equilibrium and mixing. Contrib Mineral Petrol 70:111–125

Weast RC (ed.) (1972) Handbook of Chemistry and physics. The Chemical Rubber Company, Cleveland, Ohio [52nd edn]

Zhu C, Sverjensky DA (1991) Partitioning of F-Cl-OH between minerals and hydrothermal fluids. Geochim Cosmochim Acta 55:1837–1858